Geophysical Prospecting, 2000, 48, 745–761

Detection and identification of north–south trending magnetic structures near the magnetic equator

Les P. Beard[1]

Abstract

Long, structurally undeformed north–south trending structures show no magnetic anomaly at the magnetic equator, except at the north and south truncations of the structure. However, folding, faulting, differential erosion or other structural deformation can produce detectable magnetic anomalies in a generally north–south trending equatorial structure. Spatial variation in magnetic susceptibility or remanent magnetization can also produce anomalies in equatorial north–south structures. These anomaly patterns are often more complicated than patterns produced by similar structures at high latitudes, but interpretational insight can be gained through numerical modelling of common structures. Reduction-to-pole and analytic signal filters can aid in interpretation of equatorial anomalies, but these must be applied carefully because of instabilities deriving from filter design and noise amplification.

Introduction

Interpretation of magnetic data near the magnetic equator (hereafter called simply 'equator') is complicated by several factors, one of which is that the ambient field is horizontal. This produces effects not often seen in high latitude magnetic data. Bodies that are elongate in the direction of the ambient field declination, which is usually within 5° of north at the equator (Telford, Geldart and Sheriff 1990), will show no anomalous field. In essence, long north–south striking bodies are magnetically invisible at the equator. This is true in theory only for two-dimensional bodies aligned along the nearly north–south declination at the equator. Three-dimensional elongate bodies show anomalies at north and south truncations, and also may have broad, weak negative anomalies over the centre of the body. In practice, however, this smaller central anomaly is usually obscured by geological heterogeneity.

Paper presented at the 61st EAGE Conference – Geophysical Division, Helsinki, Finland, June 1999. Received July 1999, revision accepted February 2000.
[1] Geological Survey of Norway, Leiv Eirikssons vei 39, N-7491 Trondheim, Norway.

Nevertheless, an elongate north–south striking structure may produce detectable magnetic anomalies along its length if it has some three-dimensional geological element. Structures such as faults, folds, alternating thick and thin zones (pinch-and-swell structures) or horst-and-grabens can produce detectable anomalies. Spatial variation in the magnetic susceptibility of the structure may also produce sufficient contrast for a detectable magnetic anomaly. Another parameter sometimes important in determining whether a north–south structure is magnetically detectable is remanent magnetization.

In this study, the response of elongate 3D north–south trending structures at low magnetic latitudes is modelled to determine under what conditions it is possible to detect these structures using magnetometry. By understanding the factors which allow detection of the structures, the field geophysicist is better able to design magnetic surveys to take advantage of these factors, thus enhancing the possibility for correct interpretation. It is important to be able to identify structural patterns from equatorial anomalies before they have been subjected to reduction-to-pole (RTP) or other forms of filtering.

The synthetic data were generated using survey parameters typical of a high-resolution fixed wing or helicopter survey. The reader should be aware that the model and survey dimensions are scalable without affecting results, and that the conclusions drawn apply equally to ground and aerial magnetic surveys.

Theory

The synthetic anomalies were computed by summing the responses of multiple right vertical prisms. Bhattacharyya (1964) derived an equation for the magnetic anomaly caused by a uniformly magnetized right vertical prism having infinite depth extent. By computing the response of two identical prisms, one with its top surface at depth z_1, the other at depth z_2, the magnetic anomaly of a finite prism of thickness $z_2 - z_1$ (the z-axis is positive downwards) is obtained. The expression assumes a constant ambient field over the body and allows for both induced and remanent magnetism. Following the notation of Blakely (1995), the magnetic anomaly ΔT of a semi-infinite prism parallel to the x-, y- and z-axes, located between x_1 and x_2 and y_1 and y_2, and buried at a depth z_1 is given by

$$\begin{aligned}\Delta T = C_m M\Big[&0.5\star\alpha_{23}\star\log((r-x')/(r+x')) + 0.5\star\alpha_{13}\star\log((r-y')/(r+y')) \\ &-\alpha_{12}\star\log(r+z_1) - \hat{M}_x\hat{F}_x\arctan(x'y'/(x'^2+rz_1+z_1^2)) \\ &-\hat{M}_y\hat{F}_y\arctan(x'y'/(r^2+rz_1+x'^2)) - \hat{M}_z\hat{F}_z\arctan(x'y'/(rz_1))\Big]\Big|_{x=x_1}^{x=x_2}\Big|_{y=y_1}^{y=y_2},\end{aligned} \tag{1}$$

where the ambient field direction is $\hat{\mathbf{F}} = (F_x, F_y, F_z)$ and the magnetization of the body is $\mathbf{M} = M(\mathbf{i}\hat{M}_x + \mathbf{j}\hat{M}_y + \mathbf{k}\hat{M}_z)$. The constant $C_m = \mu_0/4\pi$ in the SI system,

$$\alpha_{12} = \hat{M}_x\hat{F}_y + \hat{M}_y\hat{F}_x, \alpha_{13} = \hat{M}_x\hat{F}_z + \hat{M}_z\hat{F}_x, \alpha_{23} = \hat{M}_y\hat{F}_z + \hat{M}_z\hat{F}_y \text{ and}$$

$$r^2 = x'^2 + y'^2 + z_1'^2.$$

Blakely (1995) offers a subroutine for these expressions that allows the prism to be rotated about a vertical axis.

Detecting and identifying north–south trending structures

A two-dimensional (2D) structure, uniformly magnetized by induction and orientated along the declination direction in a horizontal ambient magnetic field, produces no magnetic anomaly (Breiner 1973). At the earth's magnetic equator, the declination is, except in rare instances, within about 5° of true north. This is thought to effectively preclude detection of long, north–south striking structures near the magnetic equator. However, the situation, though sometimes admittedly desperate, need not be thought hopeless. A few things work in the geophysicist's favour. Firstly, there are no truly 2D structures. One can always find bounds of some sort on geological structures. These bounds, at their north and south ends, can produce sizable anomalies, easily detectable (but also easily misidentified) in a magnetic survey. Secondly, geological processes often produce structures that, although they may strike generally north–south, also possess displacements, either vertically or east–west, which can produce detectable anomalies. These displacements can take the form of offsets produced by lateral or normal faulting, by erosion or by folding, to name a few. If the scales of these displacements are amenable to ground or airborne magnetic surveys, these anomalies can be identified and the north–south feature deduced. Thirdly, even if there are no displacements along the strike of an elongate north–south trending structure, it may still be possible to detect the structure if the magnetization is non-uniform along its length, or if the structure has significant remanent magnetization.

Elongate prism–truncation effects

At the equator, the induction-only magnetic anomaly of a north–south orientated vertical prism consists of a broad, weak, usually undetectable, magnetic low along the strike of the anomaly with much stronger anomalies at the north and south terminations (truncation anomalies). Consider the example of a vertical basaltic dike at the equator having a magnetic susceptibility of fairly magnetic basalt, about 0.07 SI (Clark 1997). The dike, shown in Fig. 1, has a north–south length of 6000 m, an east–west width of 200 m and a depth extent of 1000 m. The dike outcrops at the earth's surface. The north termination of the dike is vertical. In the south, the dike ramps downwards 300 m over a horizontal length of 600 m at a dip angle of 26.6°. The simulated airborne survey is at constant height of 200 m above ground level, and east–west flight lines are 200 m apart. The ambient field has a magnitude of

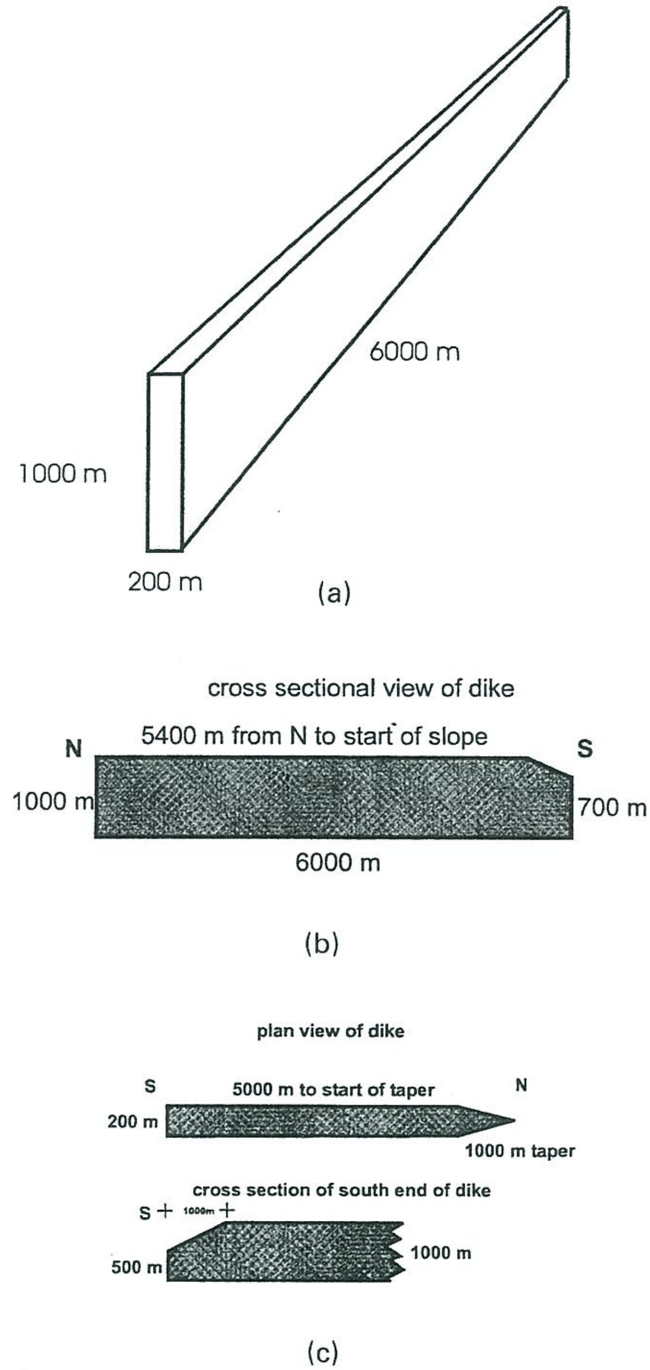

Figure 1. North–south magnetic dike models. Magnetic susceptibility = 0.07 SI. (a) Undeformed dike dimensions. (b) Cross-section of dike with sloping surface at south end. (c) Cross-section and plan view of dike with tapered truncation at north end and sloping truncation at south end.

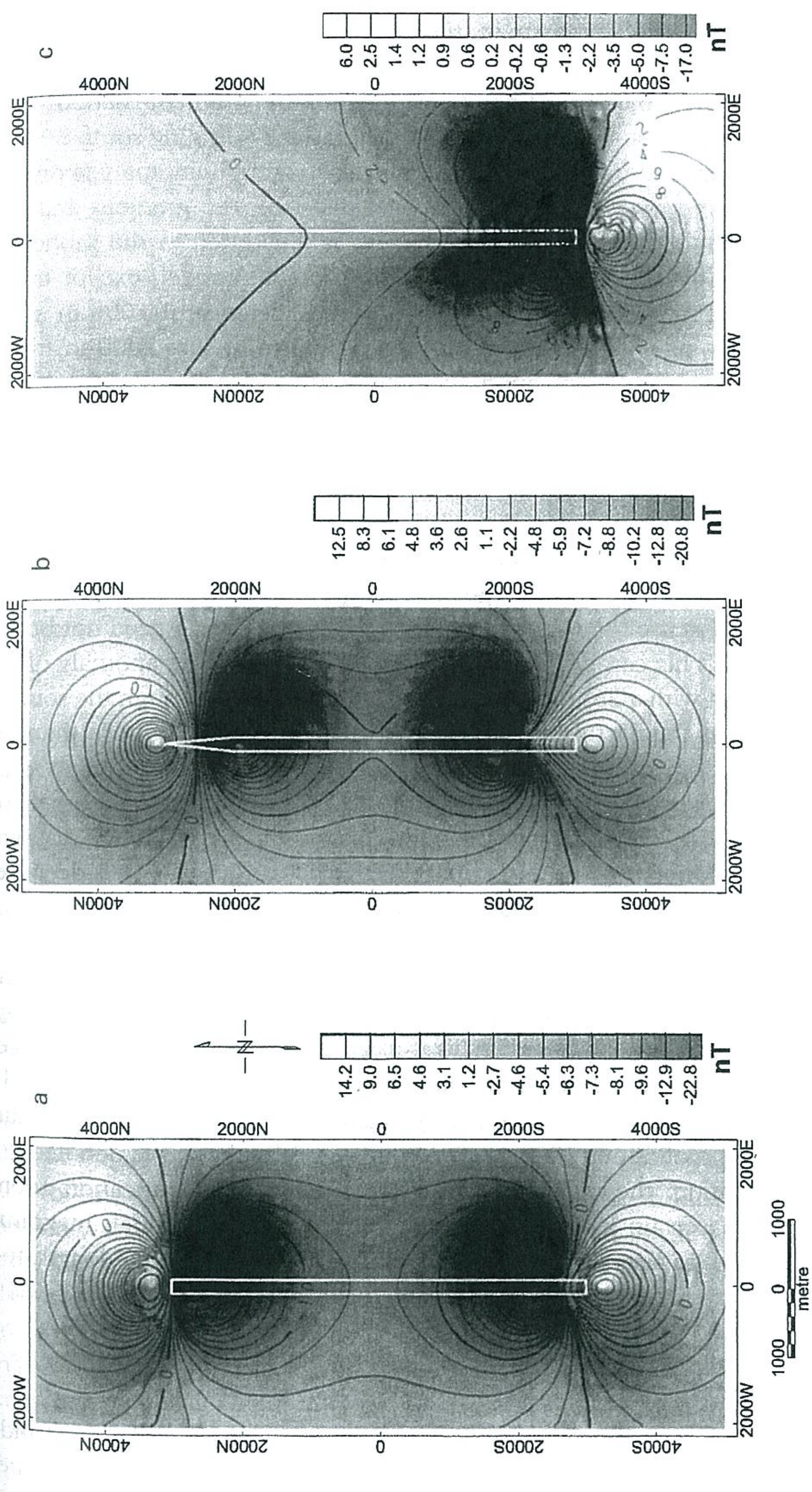

Figure 2. Truncation anomalies. (a) From dike model in Fig. 1b. (b) From dike model in Fig. 1c. (c) From dike with 26° dip to north.

35 000 nT, an inclination of 0° (horizontal), and a declination of 0° (north). The anomaly from this body is shown in Fig. 2a. Across the centre of the body, an indistinguishable magnetic low of −8 nT is produced. However, high gradients occur at both terminations. At the abrupt north termination, the gradient is about 0.2 nT/m with a peak-to-trough anomaly of 103 nT. At the gradually dipping south termination, the gradient is reduced to 0.07 nT/m and the peak-to-trough anomaly is only 78 nT. Had the dip occurred over a longer horizontal distance, the gradient and peak-to-trough anomaly would be further reduced. This is illustrated in the model used to generate Fig. 2b. This model is identical to the previous model, except that at the south end the body ramps downwards 500 m over a distance of 1000 m and at the north end the body pinches out from a width of 200 m at $y = 2000$ m to 20 m at $y = 3000$ m. The peak-to-trough anomaly at the south end is 68 nT with a gradient of 0.05 nT/m. The north pinch-out produces a peak-to-trough anomaly of 64 nT and a gradient of 0.05 nT/m. A major difference between the pinch-out and the abrupt truncation in Fig. 2a is the location of the crossover (zero equipotential contour). In Fig. 2a it occurs at the truncation, $y = 3000$ m, whereas in the pinch-out model it occurs at $y = 2500$ m. Otherwise the two north end anomalies are almost identical.

If the north–south trending structure has a dip, one of the ends may be buried deeply enough to obscure its truncation anomaly. The dip angle need not be extreme if the body is long. This can be seen in Fig. 2c, which shows the anomaly of the dike shown in Fig. 1, but with a 26° dip downwards to the north. Although the south end of the dike outcrops at the earth's surface, the north end is buried more than 2600 m deep and produces almost no anomaly. Only the south truncation anomaly is present in Fig. 2c, but the direction of dip can be inferred from the polarity of the truncation anomaly. Furthermore, the characteristic high–low anomaly pair can be distinguished from anomalies produced by more compact 3D structures that have a deep negative lobe over the body and two smaller high anomalies at both the north and south ends of the compact structure as shown by Pearson (1998).

Once a north–south trending dike exceeds a certain length-to-width ratio, the amplitude of the positive anomaly just off the end of the dike is equal to the amplitude of the paired negative anomaly over the dike. The negative anomaly will be larger than the positive anomaly in amplitude if the dike has a small length-to-width ratio. For the dike described in Fig. 1a, the positive and negative amplitudes become equal at a length-to-width ratio of about 20:1, as shown in Fig. 3 by the curve denoted $|\text{high}| - |\text{low}|$. In addition, the magnitude of the peak-to-trough truncation anomaly is constant beyond a certain length-to-width ratio. The peak-to-trough magnitude for the example in Fig. 1a becomes constant at about 200 nT when the length-to-width ratio exceeds about 15:1, as shown in Fig. 3 by the curve denoted $|\text{high}| + |\text{low}|$.

Faulted or folded structures

An elongate structure may have a predominant north–south strike, but folding or faulting may produce enough east–west (or vertical) displacement to produce a

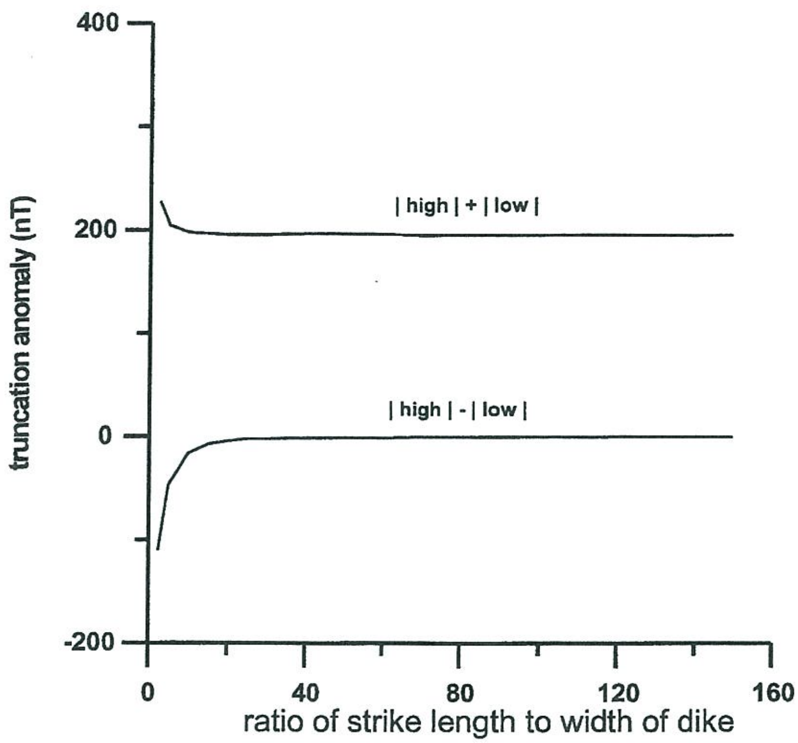

igure 3. Effect of dike's length-to-width ratio on shape and magnitude of truncation anomaly.

etectable anomaly. The anomaly patterns can be subtle and complicated. An nderstanding of the patterns produced by simple models can aid in identification of imilar structures in the field. The various structures modelled in this section are ased on the dimensions of the prism in Fig. 1a, but have been distorted by folding or aulting.

Figure 4a shows the anomaly produced by a dike folded by north–south ompression with vertical fold axes. The wavelength of the fold is 3200 m, and it as a peak-to-trough displacement of 400 m. This produces a 14° fold angle. The nomaly directly over the body is weakly negative, about −15 nT, and it resembles the olded source structure. Easily detectable positive–negative anomaly pairs in excess of 0 nT (peak-to-trough) are created at the minima and maxima of the fold. Therefore, appears that even modest folding of magnetic structures should produce detectable nomalies at the equator.

Figure 4b shows the anomaly produced by a dike folded by north–south ompression with horizontal, east–west fold axes. A peak of the folded dike touches he surface at $y = 100$ m and is at a maximum of 200 m below the surface at = 1900 m and $y = 2100$ m. This implies a 4000 m wavelength and a gradual fold ngle of 5.7°. This structure produces a distinctive pattern – a strong negative −30 nT) where the dike reaches the surface, which increases to about −4 nT where he dike is most deeply buried. The largest anomalies are still at the north and south runcations. The equatorial position is advantageous in this case, for the undulations n a similar structure at high latitudes would be less apparent.

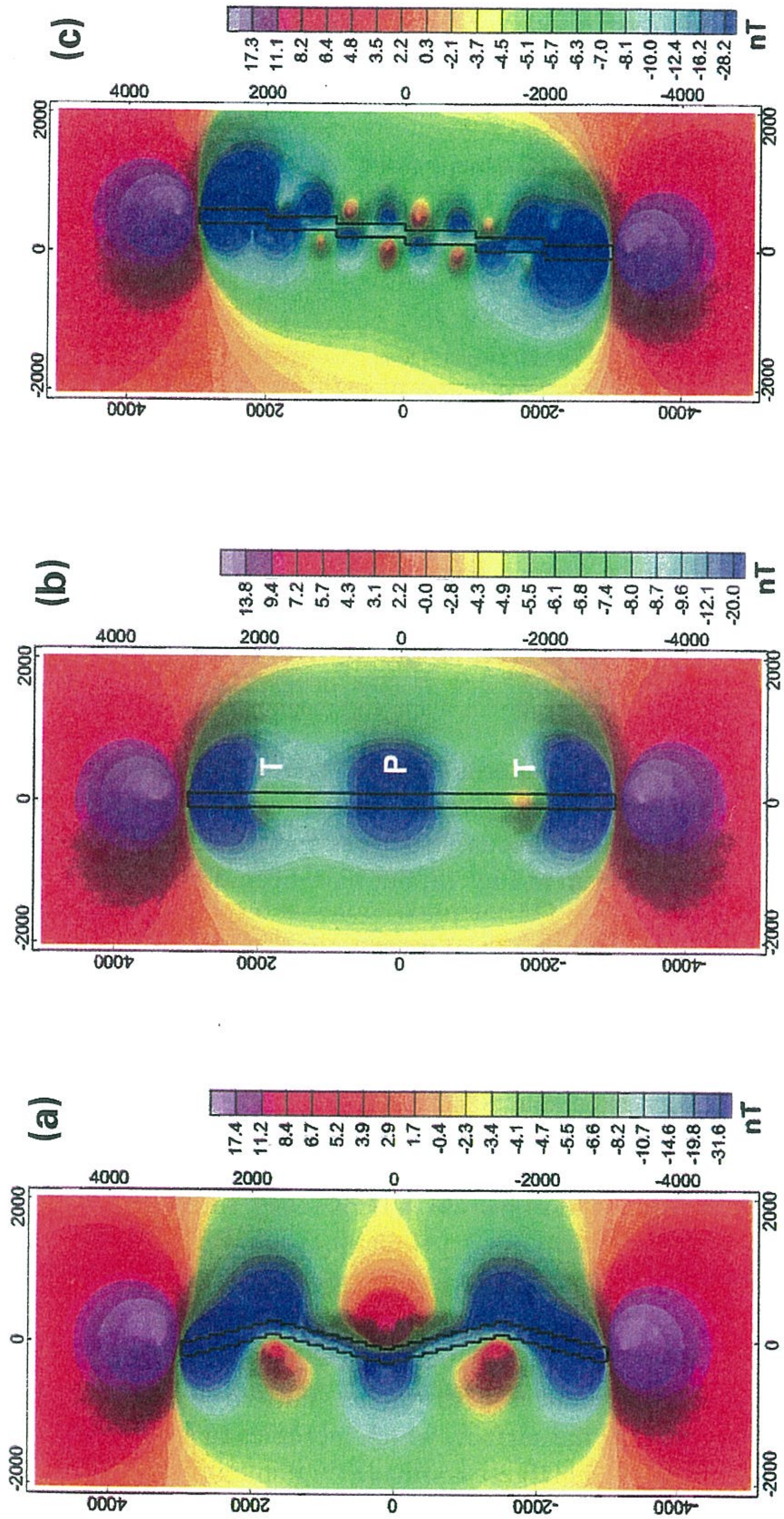

Figure 4. Anomalies produced by structural deformations. (a) Laterally folded dike. (b) Vertically folded dike (P = peak/crest of fold, T = trough). (c) Strike-slip faulted dike.

Other deformations or variations may produce anomalies similar to that of the model in Fig. 4b. If an elongate magnetized body varies in thickness, as with pinch-and-swell structures (Price and Cosgrove 1990), an alternating high–low anomaly pattern similar to Fig. 4b will be produced. The highs would occur over the narrow parts of the structure, the lows over the widest parts. Similarly, if the elongate body outcrops and is eroded, anomalous lows would occur over the uneroded peaks and highs over the erosional valleys. The same applies for horst-and-graben structures. Anomalous highs would appear over the grabens and lows over the horsts. Variations in magnetic susceptibility along the length of a north–south elongate structure can also produce anomalies similar to that in Fig. 4b. Magnetic lows would occur over areas of high susceptibility and highs over low-susceptibility zones.

East–west strike-slip faulting may produce en-echelon offsets in a north–south trending structure. Figure 4c shows the complicated anomaly pattern produced when a dike is displaced in the manner shown. Where a segment of the dike is offset from an adjacent segment, two anomalies are produced – a negative anomaly over the dike (in this example, about −17 nT) and a relatively small positive anomaly on the opposite side of the fault. These fairly small anomalies could be hard to detect if moderate, near-surface geological variation is present. However, larger east–west offsets would produce correspondingly larger anomalies.

Effects of remanent magnetization

Even if remanent magnetization dominates the magnetic response of a straight, north–south trending structure, this remanence can be difficult to distinguish at the equator. The main effect of most remanent magnetization orientations on the anomaly produced by the dike in Fig. 1 is to increase or decrease the north and south termination anomalies and to rotate them. Figures 5a and b show the effects of two very different remanent magnetization orientations. In both cases, the dike has a susceptibility of 0.07 and a Koenigsberger ratio of 5.0 (i.e. remanence dominates induced magnetism by a factor of 5). Figure 5a shows the anomaly produced when the remanent magnetization has an inclination of 20° up and a declination of 110° (20°S from E). An inclination of 40° down and a declination of 300° (30°N from W) produce the anomaly shown in Fig. 5b. The anomaly patterns are similar for both remanent magnetization orientations, the main difference being a rotation of the truncation anomalies. In both examples, the central part of the dike shows no detectable anomaly, as in the pure induction case.

On the other hand, if the north–south structure is folded and remanent magnetization dominates the response, the anomaly may be noticeably altered from the pure induction anomaly. Figure 6 shows the total field anomaly produced by the same folded dike as in Fig. 4a, but with remanent magnetization dominant. The susceptibility and remanence magnitude and direction are the same as in Fig. 5a. Compare the anomaly in Fig. 6 with the induction-only anomaly in Fig. 4a. In the case of Fig. 6, remanence has increased the magnitude of the anomalies and has

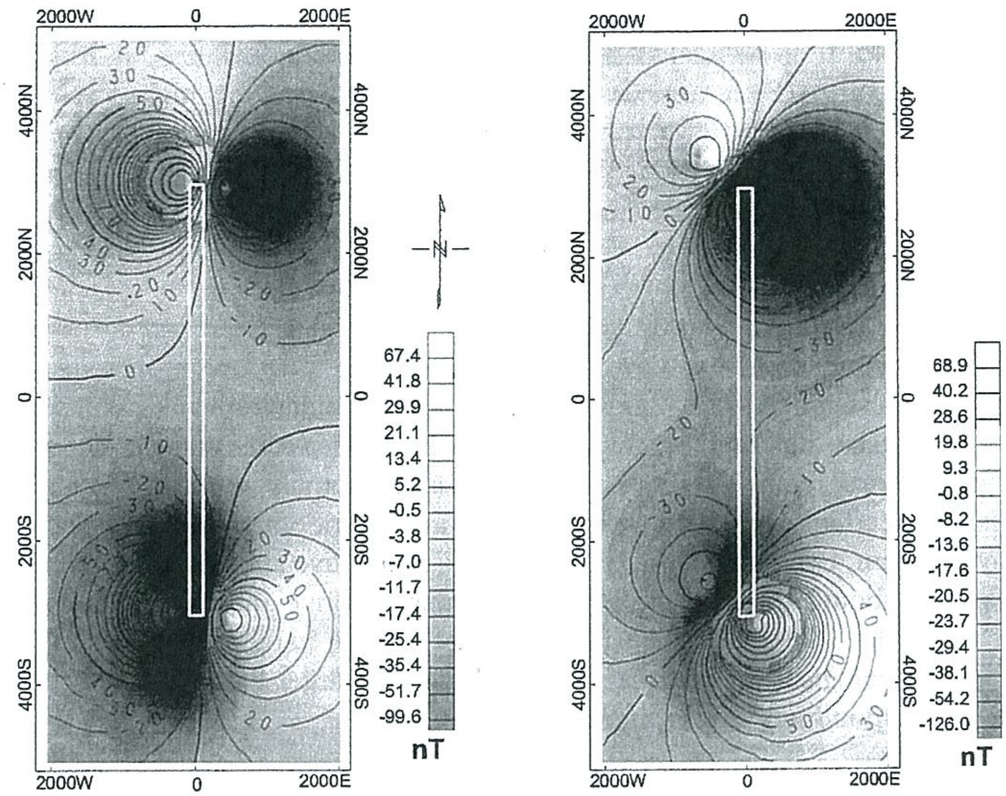

(a) (b)

Figure 5. Effect of remanent magnetization on truncation anomaly. Koenigsberger ratio = 5. (a) Remanence direction: inclination = 20° up, declination = 110° clockwise from north. (b) Remanence direction: inclination = 40° down, declination = 300° clockwise from north.

caused parts of the fold trending approximately NNW–SSE to have a positive anomaly. In the pure induction case a negative anomaly is associated with the entirety of the folded structure.

Although the effect of remanent magnetization is to rotate the truncation anomalies, it is evidently not the only phenomenon capable of this. Anisotropy has also been shown to rotate magnetic anomalies (Florio *et al.* 1993). However, in most rocks, the degree of anisotropy is not high enough to influence the shape of the anomaly. Banded iron formations and ores containing phyrrotite with strong preferred direction are important exceptions (Clark 1997). Further study should be done to understand the effects of anisotropy on low latitude anomalies.

Aliasing and flight direction considerations

Undersampling can be a problem anywhere geophysical data are collected, and in general, this problem is no more severe for magnetic surveys at low latitudes than at high latitudes. The anomalies in Fig. 4a are of sufficiently long wavelength that they

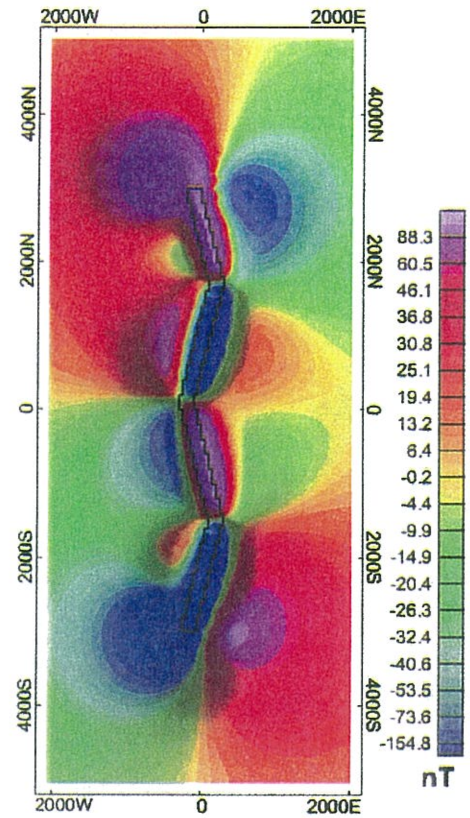

Figure 6. Effect of dominant remanent magnetization on anomaly from a laterally folded dike.

would still be evident on surveys with larger line separations than the 200 m spacing used to create the survey data. Figure 7a shows the anomaly of the same folded dike as in Fig. 4a, but now with a line separation of 1000 m. As in Fig. 4a, the flight direction is east–west. Clearly, some detail has been lost. In comparison with Fig. 4a, east–west gradients are less pronounced. However, the strong gradients in the north–south direction are maintained at either end of the dike. This suggests there might be some advantage in acquiring data along north–south flight lines instead of east–west lines, even though the east–west direction is suggested by the strike direction of the dike. Figure 7b shows the anomaly obtained if a 1000 m spacing is used with a north–south line direction. From the gridded data from the north–south flight lines, the suggestion of a fold structure is more evident, and the truncation anomalies are less distorted than with the 1000 m east–west data.

Reduction-to-pole and other transformations

This paper is not intended to analyse the merits or deficiencies of the various reduction-to-pole (RTP) techniques that have sought to overcome the low latitude instabilities of the standard RTP filter using a Fourier transform approach (Blakely 1995). Silva (1986) and Hansen and Pawlowski (1989) have designed transform

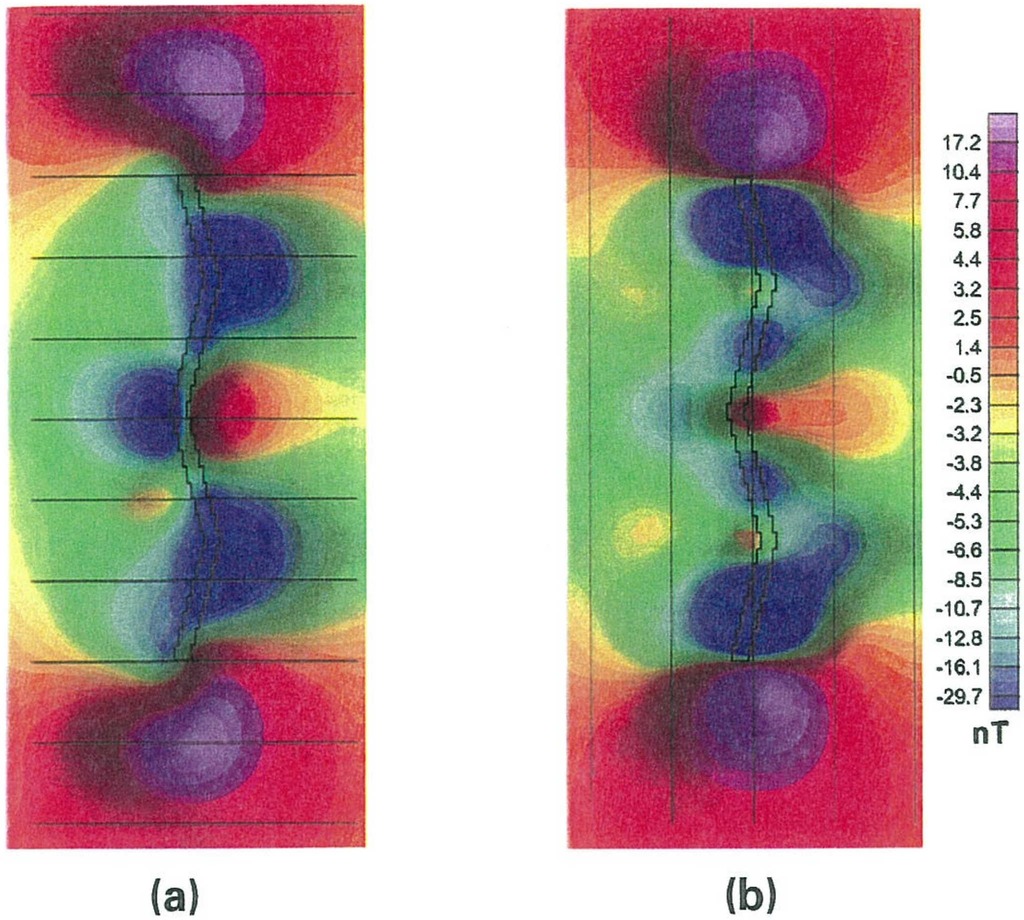

Figure 7. Effects of aliasing on anomaly shown in Fig. 3a. (a) East–west flight line direction, 1000 m line spacing. (b) North–south flight line direction, 1000 m line spacing.

techniques specifically for low latitudes. Irrespective of the technique used, the transform of the anomaly of a purely north–south striking structure with no lateral or vertical deformation will be problematic. However, if some vertical or lateral deformation is present, interpretation may be improved by careful application of a modified Fourier transform RTP filter. The modified filter uses in the amplitude component of the filter an inclination of higher latitude than the actual inclination. This reduces filter instability, but underestimates the amplitudes of north–south features (Geosoft, Inc. 1996). Although this amplitude underestimation will create inaccuracies in depth-to-source estimates, the transformed anomaly may nevertheless

Figure 8. Effects of filters on anomalies from a laterally folded dike, both with and without remanence. (a) Reduction-to-pole filter applied to induction-only anomaly in Fig. 4a. (b) Analytic signal applied to Fig. 4a anomaly. (c) Reduction-to-pole anomaly applied to remanence-dominated anomaly in Fig. 6. (d) Analytic signal applied to Fig. 6 anomaly.

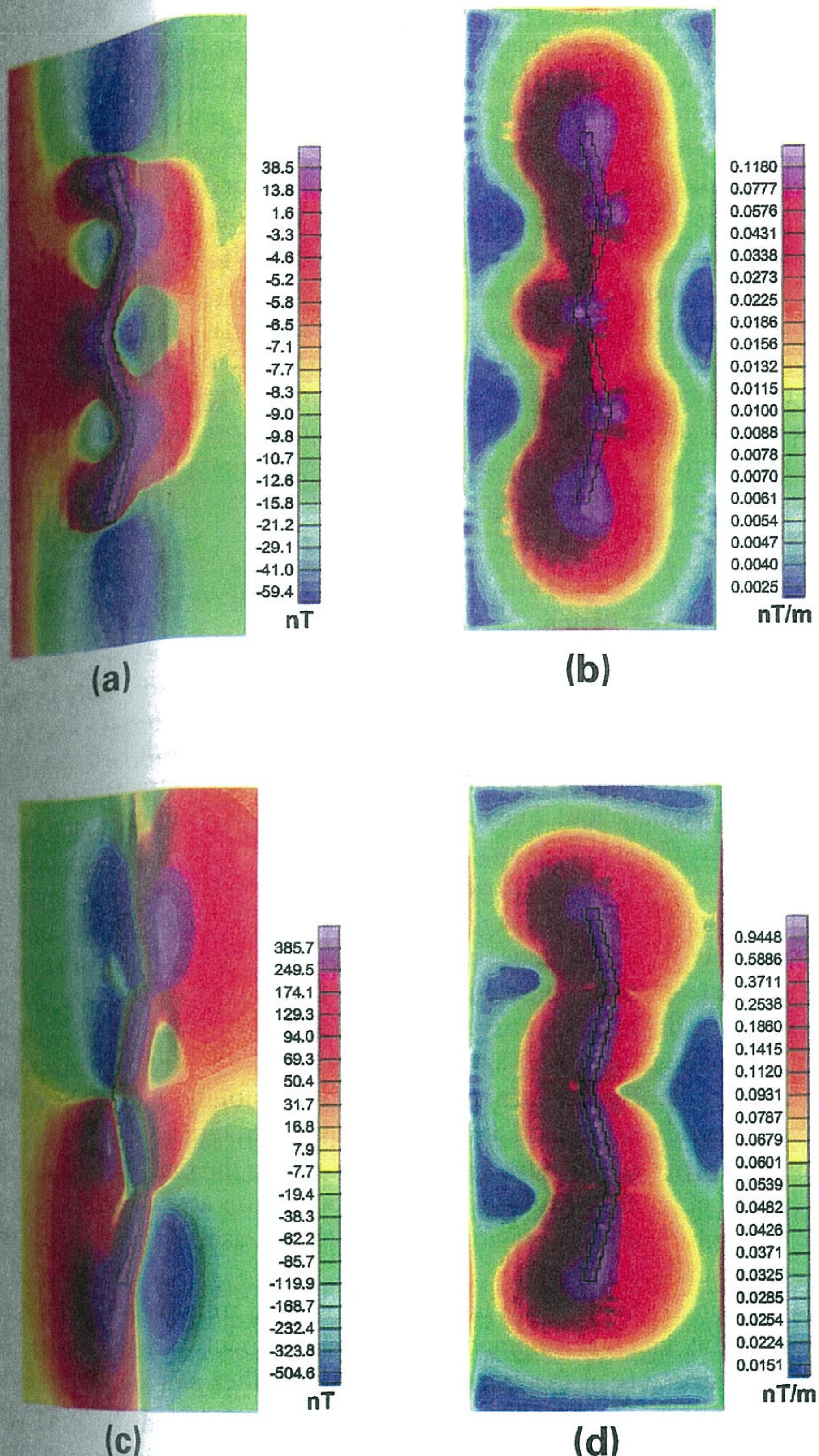
38.5
13.8
1.6
-3.3
-4.6
-5.2
-5.8
-6.5
-7.1
-7.7
-8.3
-9.0
-9.8
-10.7
-12.6
-15.8
-21.2
-29.1
-41.0
-59.4
nT
(a)
0.1180
0.0777
0.0576
0.0431
0.0338
0.0273
0.0225
0.0186
0.0156
0.0132
0.0115
0.0100
0.0088
0.0078
0.0070
0.0061
0.0054
0.0047
0.0040
0.0025
nT/m
(b)
385.7
249.5
174.1
129.3
94.0
69.3
50.4
31.7
16.8
7.9
-7.7
-19.4
-38.3
-62.2
-85.7
-119.9
-168.7
-232.4
-323.8
-504.6
nT
(c)
0.9448
0.5886
0.3711
0.2538
0.1860
0.1415
0.1120
0.0931
0.0787
0.0679
0.0601
0.0539
0.0482
0.0426
0.0371
0.0325
0.0285
0.0254
0.0224
0.0151
nT/m
(d)

resemble the source structure(s) more closely than the original data. An example is the RTP transformation of the anomaly shown in Fig. 4a. The shape of the folded dike is more distinct in the RTP transformation, shown in Fig. 8a. However, if remanent magnetism dominates the response and this remanence is not taken into consideration in the RTP transformation, results may be unsatisfactory. Figure 8c shows the RTP transformation of the remanence-dominated folded dike anomaly shown in Fig. 6. Remanence was not taken into account in the application of the RTP filter. In this example there is clearly no advantage in using an RTP filter.

MacLeod, Jones and Dai (1993) and Qin (1994) recognized the limitations of using RTP filters at low latitudes and suggested the use of the 3D analytic signal as an aid in interpreting low latitude magnetic data. Figures 8b and d show the 3D analytic signal applied to the anomalies in Figs 4a and 6, respectively. The fold structure is especially clear in the case of the analytic signal of the remanence-dominated anomaly (Fig. 8d). The remanence produced strong east–west gradients along the edges of the folded dike and therefore produces a strong analytic signal in these areas, clearly outlining the folds.

Field example – West Africa

Figure 9a shows a subset of aeromagnetic data from a survey in Burkina Faso, West Africa. Two positive–negative pairs are labelled X and Y. Could either of these anomalies represent truncation anomalies from north–south trending magnetic structures? Anomaly X has a pronounced magnetic high immediately to the south of a nearly equal magnetic low. The magnetic field climbs gradually to the background towards the north. Figure 9b shows a profile across anomaly X in the direction of declination. The profile bears close resemblance in shape and magnitude to a synthetic profile across the south end of the same elongate north–south prism shown in Fig. 1, and having a magnetic susceptibility of 0.03 SI units. The north end truncation anomaly does not appear in the data. This could be because the structure extends beyond the limits of the survey area, or because the structure is dipping. The crest of the magnetic anomaly is slightly smaller than the trough, consistent with the anomaly pattern of a dipping structure. A third possibility is that the structure is actually equidimensional, but with dominant remanent magnetization. In this case, the direction of remanent magnetization would have to be in the direction of declination, a few degrees west of north, and down at about 45°. In the absence of clear geological indicators, petrophysical and gravity data would be useful in determining which hypothesis is most likely.

Anomaly Y is an anomaly which falls off sharply to a minimum, then rises sharply again. This is the kind of anomaly one would expect to see from a laterally equidimensional structure at the magnetic equator (Barker 1975). Compare a profile across anomaly Y (Fig. 9c) with the synthetic anomaly of a laterally equidimensional pipe (Fig. 9d) having lateral dimensions 200 m by 200 m, a depth extent of 1000 m and a susceptibility of 0.03 SI units. The close resemblance between the two makes it

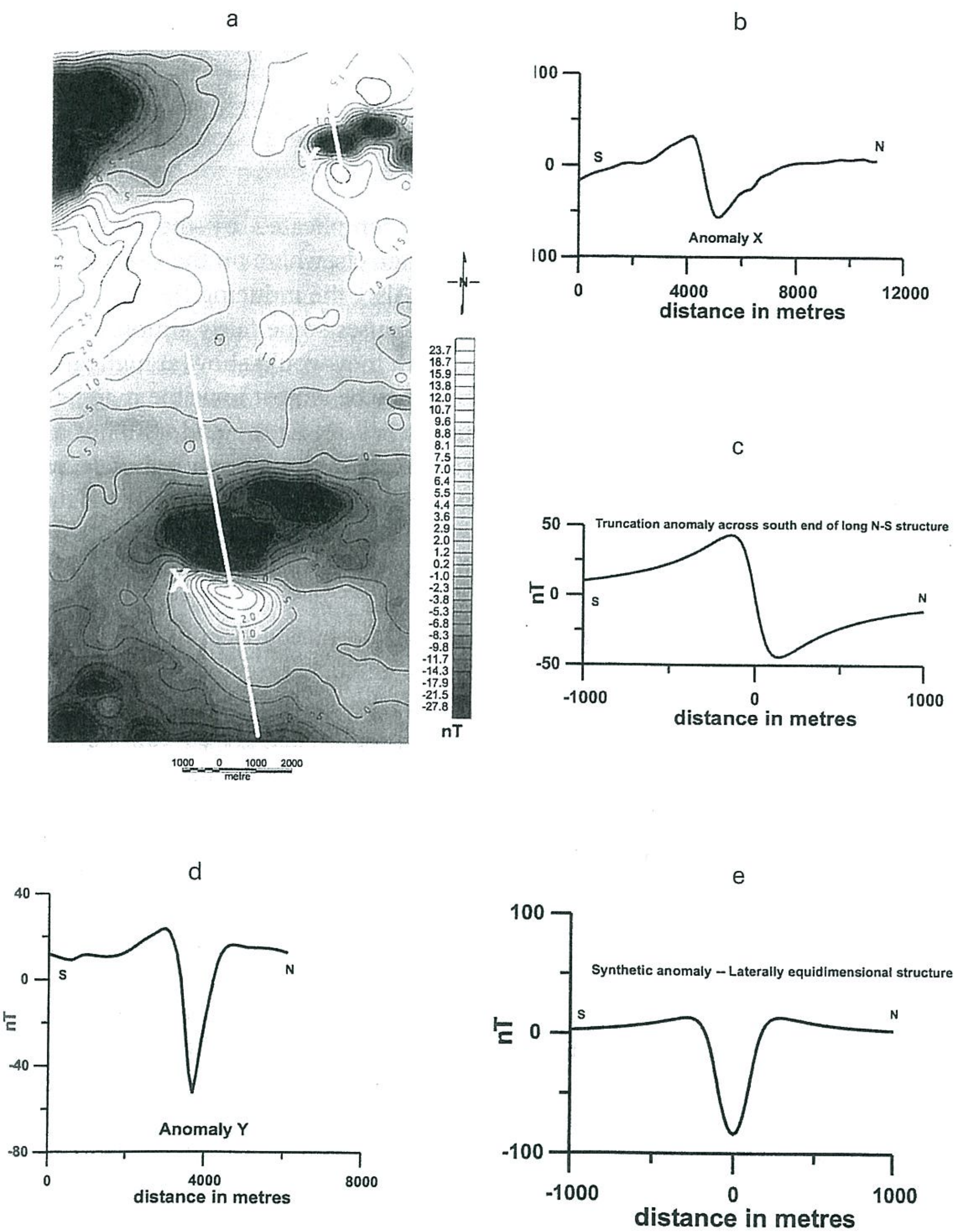

Figure 9. Aeromagnetic anomalies from Burkina Faso, West Africa. (a) Aeromagnetic data showing anomalies X and Y and profile paths. (b) Profile over anomaly X. (c) Synthetic profile over south termination of a long north–south structure. (d) Profile over anomaly Y. (e) Synthetic profile over laterally equidimensional vertical pipe.

highly unlikely that this is the truncation anomaly of a long north–south trending structure, but is rather a laterally equidimensional structure.

Discussion and conclusions

Interpretation of low latitude magnetic data is complicated by the fact that the inducing field is weaker at the magnetic equator than elsewhere on the earth's surface, thus producing anomalies of smaller magnitude. Also, the inducing field is parallel to the earth's surface at the magnetic equator. This causes some fairly simple structures to have more complicated magnetic anomalies than they would show at high latitudes. Long, straight, north–south trending structures may be almost invisible magnetically, except at the north and south endpoints of the structure. At the endpoints of a body that is magnetic relative to its host rock, a sizable peak-to-trough anomaly will be produced having a characteristic shape – a positive anomaly off or nearly off the end of the body and a negative anomaly of the same magnitude on the body. The reverse pattern would be seen if the north–south structure was non-magnetic relative to more magnetic host rock.

Even slight dips can cause one of the ends to be buried deeply enough for its truncation anomaly to become undetectable, and in such cases only one truncation anomaly may appear. A dipping structure produces a truncation anomaly with a slightly different shape from that of a non-dipping structure, as can be seen in Figs 2a–c, so it may be possible to deduce a structural dip from the anomaly shape. The presence of remanent magnetization, regardless of direction, has the effect of rotating the truncation anomalies and modifying their magnitudes. A sufficient degree of anisotropy of magnetic susceptibility would be likely to have a similar effect.

Folding, faulting, differential stresses or erosion may alter long north–south structures. Geochemical differences along the length of the body may cause magnetic susceptibility differences along strike. These changes can produce detectable anomalies along the strike of the structure. These anomalies will probably be smaller in magnitude and spatial extent than the truncation anomalies at the north and south extremities. However, the patterns produced by different processes are distinct, as seen in Fig. 4, and can aid in interpretation.

Enhancement of magnetic anomalies by the use of filters is problematic when applied to long north–south equatorial structures. If no significant deformation exists along strike, the only anomalies appear at the north and south endpoints, and filtering is of little use. If folding or faulting produces an along-strike anomaly pattern, filters such as reduction-to-pole or analytic signal may be of value. Reduction-to-pole filters applied to low latitude data may be unstable, but if applied with care may aid the interpreter (Fig. 8a). However, if remanent magnetization dominates the signal and is not accounted for in the RTP operation, the filtered data can be misleading (Fig. 8c). Analytic signal filters appear to hold some advantage over RTP filters in this respect, but can be negatively affected by poorly processed or noisy data.

Acknowledgements

This study was funded by the Geological Survey of Norway. Discussions with E. Tveten and I. MacLeod and reviews by E. Eide, J.D. Fairhead and K. Kis improved the clarity of the work. I thank Paterson, Grant and Watson, Ltd and the Government of Burkina Faso for permitting the use of their aeromagnetic data.

References

Barker R.D. 1975. Elementary approximations in aeromagnetic interpretation for application in low latitudes. *Geophysics* **40**, 686–688.

Bhattacharyya B.K. 1964. Magnetic anomalies due to prism-shaped bodies of arbitrary polarization. *Geophysics* **29**, 517–531.

Blakely R.J. 1995. *Transformations in Potential Theory in Gravity and Magnetic Applications*, Ch. 12. Cambridge University Press.

Breiner S. 1973. *Applications Manual for Portable Magnetometers*. Geometrics, Palo Alto.

Clark D.A. 1997. Magnetic petrophysics and magnetic petrology: aids to geological interpretation of magnetic surveys. *AGSO Journal of Australian Geology and Geophysics* **17**, 83–103.

Florio G., Fedi M., Rapolla A., Fountain D.M. and Shive P.N. 1993. Anisotropic magnetic susceptibility in the continental lower crust and its implication for the shape of magnetic anomalies. *Geophysical Research Letters* **20**, 2623–2626.

Geosoft, Inc. 1996. *MAGMAP (FFT-2D) User Guide*. Geosoft, Inc.

Hansen R.O. and Pawlowski R.S. 1989. Reduction to pole at low latitudes by Wiener filtering. *Geophysics* **54**, 1607–1613.

MacLeod I., Jones K. and Dai T. 1993. 3-D analytic signal in the interpretation of total magnetic field data at low latitudes. *Exploration Geophysics* **24**, 679–687.

Pearson W.C. 1998. Magnetic reduction-to-the-pole at low latitudes. In: *Geological Applications of Gravity and Magnetics: Case Histories* (eds R. Gibson and P. Millegan). SEG Geophysical Reference Series No. 8. SEG, Tulsa, OK.

Price N.J. and Cosgrove J.W. 1990. *Analysis of Geological Structures*. Cambridge University Press.

Qin S. 1994. An analytic signal approach to the interpretation of total field magnetic anomalies. *Geophysical Prospecting* **42**, 665–676.

Silva B.C.J. 1986. Reduction to the pole as an inverse problem and its application to low latitude anomalies *Geophysics* **51**, 369–382.

Telford W.M., Geldart L.P. and Sheriff R.E. 1990. *Applied Geophysics,* 2nd edn. Cambridge University Press.